

## Supplementary Information For:

### Highly mesoporous SAPO-11 molecular sieves with tunable acidity: facile synthesis, formation mechanism and catalytic performance in hydroisomerization of *n*-dodecane

Shuo Tao<sup>a, b</sup>, Xiaolei Li<sup>a, b\*</sup>, Guang Lv<sup>b</sup>, Congxin Wang<sup>b</sup>, Renshun Xu<sup>b</sup>, Huaijun Ma<sup>b</sup>,  
Zhijian Tian<sup>b\*</sup>

<sup>a</sup> Shandong Provincial Key Laboratory of Chemical Energy Storage and Novel Cell  
Technology, School of Chemistry and Chemical Engineering, Liaocheng University,  
Liaocheng, Shandong 252059, China

<sup>b</sup> Dalian National Laboratory for Clean Energy, Dalian Institute of Chemical Physics,  
Chinese Academy of Sciences, Dalian, Liaoning 116023, China

**\*Corresponding author**

**Email addresses:** lixiaolei1@126.com (X. Li), tianz@dicp.ac.cn (Z. Tian)

## Figure Captions:

**Fig. S1.** TEM image of the silicoaluminophosphate dry gel.

**Fig. S2.** N<sub>2</sub> adsorption isothermal and corresponding BJH pore size distributions of (a) silicoaluminophosphate dry gel and (b) silicoaluminophosphate-organosilane composite.

**Table S1** Texture properties of the silicoaluminophosphate (SAP) dry gel and the silicoaluminophosphate-organosilane composite (SOC).

**Fig. S3.** (a) TG and (b) DSC curves of samples SAPO-11-C and SAPO-11-H1.

**Table S2** SAPO-11 acidity measurement by Py-IR at different temperatures.

**Fig. S4.** XRD patterns of the products prepared with different reaction times SAPO-11-H7 (1h), SAPO-11-H8 (3h), SAPO-11-H9 (6h), SAPO-11-H10 (9h), SAPO-11-H11 (12h) and SAPO-11-H12 (18h).

**Fig. S5.** SEM images of samples prepared with different reaction times (a), (b) SAPO-11-H8; (c), (d) SAPO-11-H9; (e), (f) SAPO-11-H10; (g), (h) SAPO-11-H11 and (i), (j) SAPO-11-H12.

**Table S3** Texture properties of the calcined samples prepared with different reaction times.

**Fig. S6.** NH<sub>3</sub>-TPD curves of products prepared with different reaction times.

**Fig. S7.** TG curves of products prepared with different reaction times.

**Fig. S8.** TEM image of the Pt/SAPO-11-H1 catalyst.

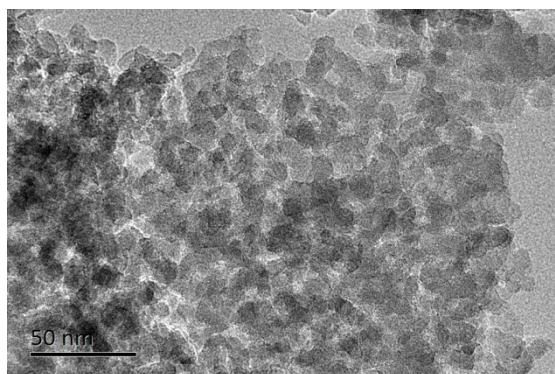


**Fig. S1.** TEM image of the silicoaluminophosphate dry gel.

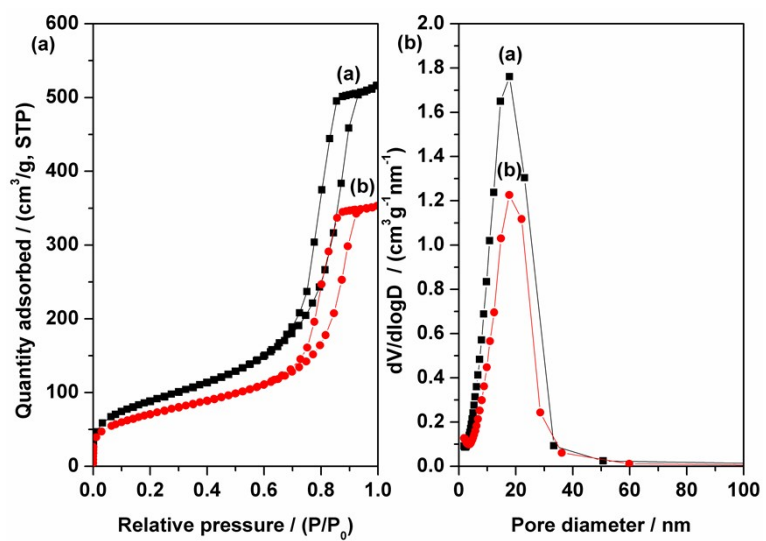
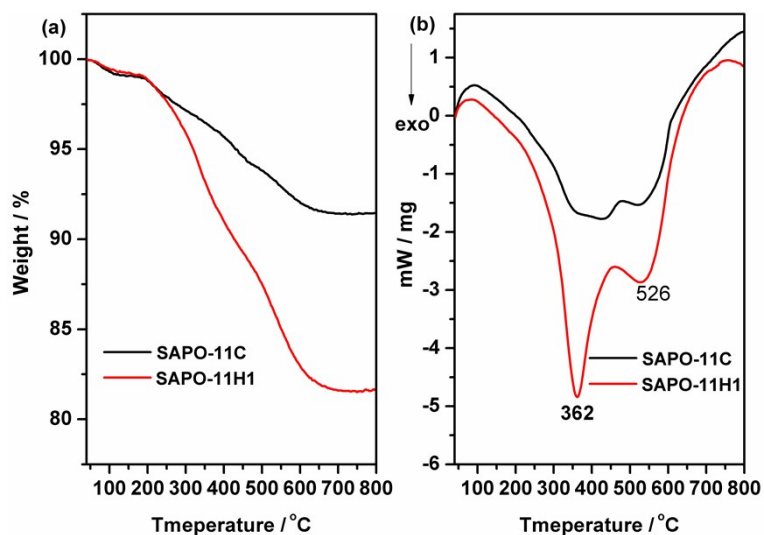


**Fig. S2.** N<sub>2</sub> adsorption isothermal and corresponding BJH pore size distributions of (a) silicoaluminophosphate dry gel and (b) silicoaluminophosphate-organosilane composite.

**Table S1** Texture properties of the silicoaluminophosphate (SAP) dry gel and the silicoaluminophosphate-organosilane composite (SOC).

Sample	Surface area /(m <sup>2</sup> /g)			Pore volume /(cm <sup>3</sup> /g)	
	S <sub>BET</sub> <sup>a</sup>	S <sub>micro</sub> <sup>b</sup>	S <sub>ext</sub> <sup>c</sup>	V <sub>total</sub>	V <sub>micro</sub> <sup>d</sup>
SAP	324	27	296	0.80	0.01
SOC	253	38	215	0.53	0.02

<sup>a</sup> BET surface area, <sup>b</sup> t-plot micropore surface area, <sup>c</sup> t-plot external surface area, <sup>d</sup> t-plot micropore volume.

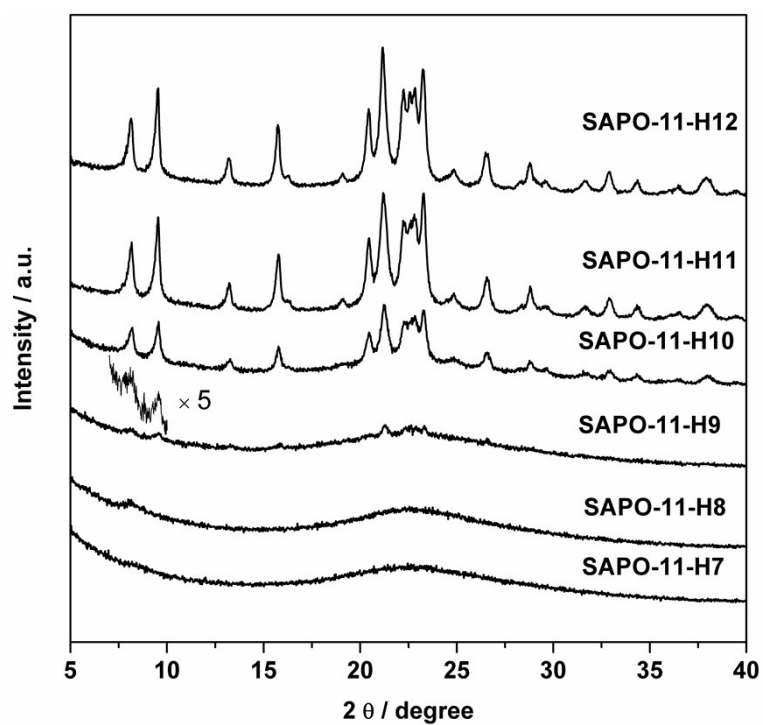


**Fig. S3.** (a) TG and (b) DSC curves of samples SAPO-11-C and SAPO-11-H1.

**Table S2**

SAPO-11 acidity measurement by Py-IR at different temperatures.

Sample	Brønsted ( $\mu\text{mol Py/g}$ )			Lewis ( $\mu\text{mol Py/g}$ )		
	150 °C	250 °C	350 °C	150 °C	250 °C	350 °C
SAPO-11-C	59.2	45.3	28.9	20.1	11.8	11.6
SAPO-11-H3	29.9	12.8	2.9	18.6	6.4	3.5
SAPO-11-H4	39.5	24.1	12.6	12.1	7.8	5.3
SAPO-11-H1	50.4	28.3	14.5	23.5	9.2	6.9
SAPO-11-H5	57.4	30.3	15.1	15.6	12.7	10.0
SAPO-11-H6	58.8	36.0	19.3	19.2	9.1	8.5

**Fig. S4.** XRD patterns of the products prepared with different reaction times SAPO-11-H7 (1h),

SAPO-11-H8 (3h), SAPO-11-H9 (6h), SAPO-11-H10 (9h), SAPO-11-H11 (12h) and SAPO-11-H12 (18h).

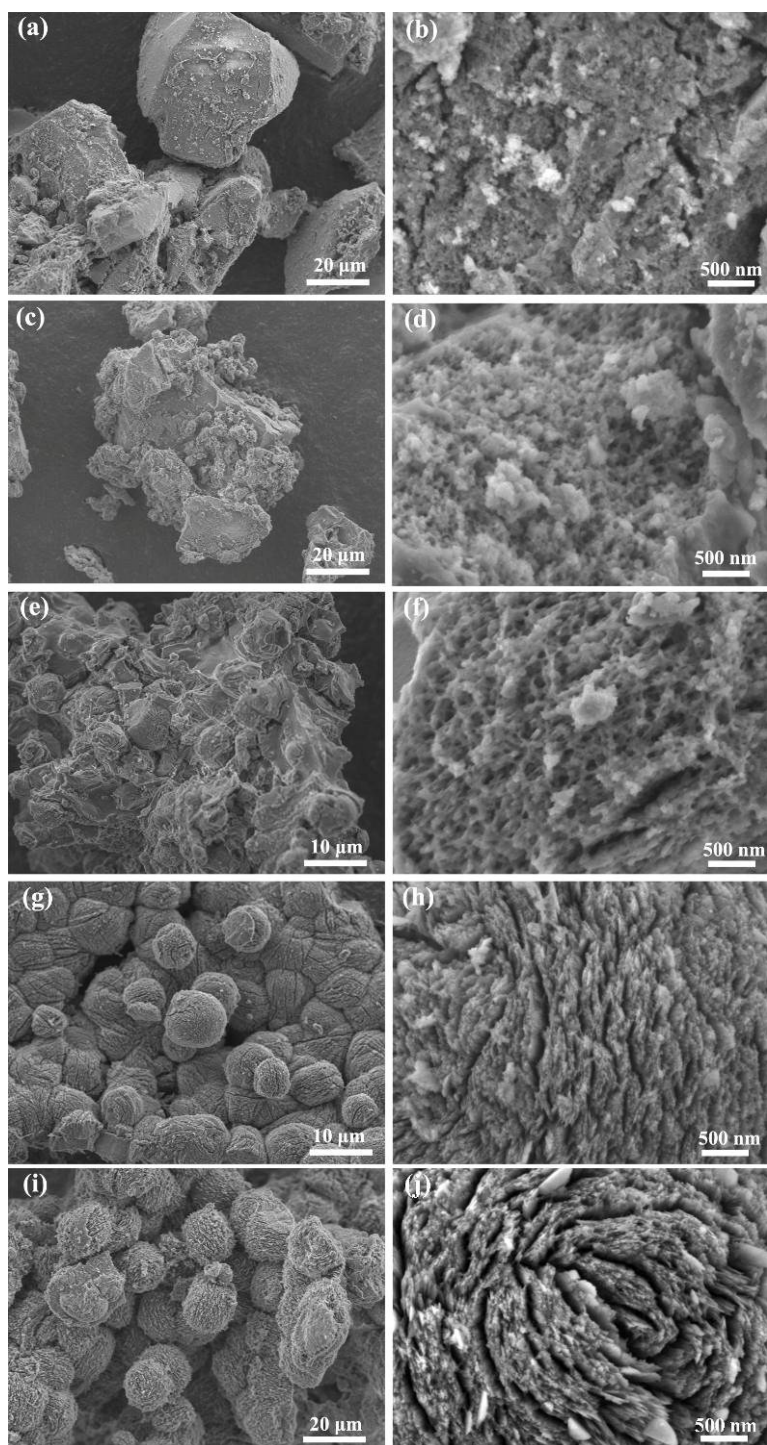


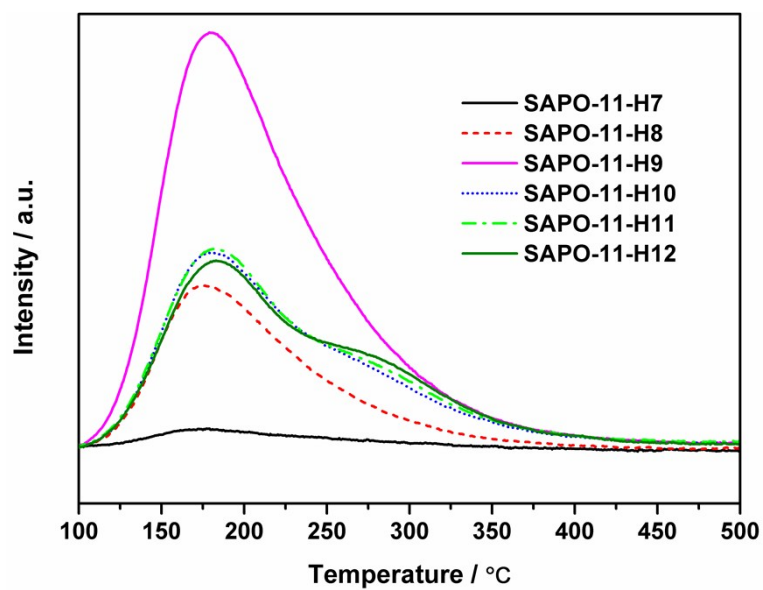
**Fig. S5.** SEM images of samples prepared with different reaction times (a), (b) SAPO-11-H8; (c), (d) SAPO-11-H9; (e), (f) SAPO-11-H10; (g), (h) SAPO-11-H11 and (i), (j) SAPO-11-H12.

**Table S3**

Texture properties of the calcined samples prepared with different reaction times.

Sample	Surface area /(m <sup>2</sup> /g)			Pore volume /(cm <sup>3</sup> /g)	
	S <sub>BET</sub> <sup>a</sup>	S <sub>micro</sub> <sup>b</sup>	S <sub>ext</sub> <sup>c</sup>	V <sub>total</sub>	V <sub>micro</sub> <sup>d</sup>
SAPO-11-H7	7.4	0.42	7.0	0	0
SAPO-11-H8	79	0	79	0.12	0
SAPO-11-H9	355	0	355	0.36	0
SAPO-11-H10	345	57	288	0.37	0.02
SAPO-11-H11	352	160	192	0.30	0.07
SAPO-11-H12	358	165	193	0.31	0.07

<sup>a</sup> BET surface area, <sup>b</sup> t-plot micropore surface area, <sup>c</sup> t-plot external surface area, <sup>d</sup> t-plot micropore volume.

**Fig. S6.** NH<sub>3</sub>-TPD curves of products prepared with different reaction times.

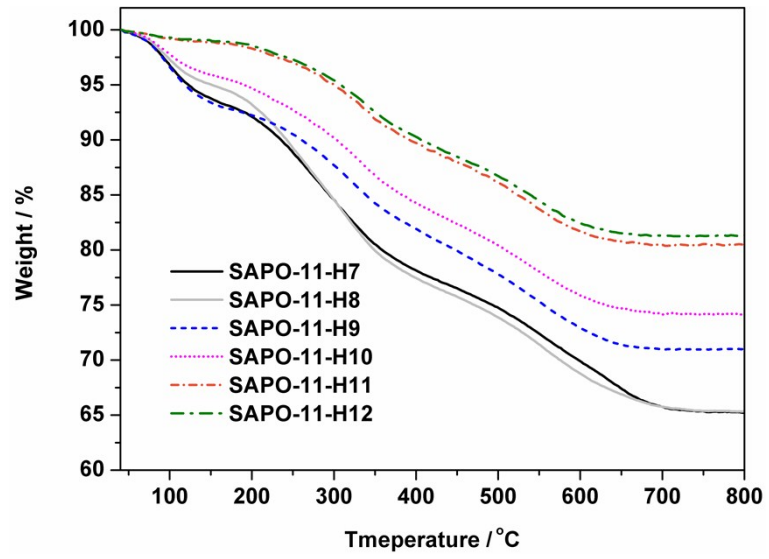


Fig. S7. TG curves of products prepared with different reaction times.

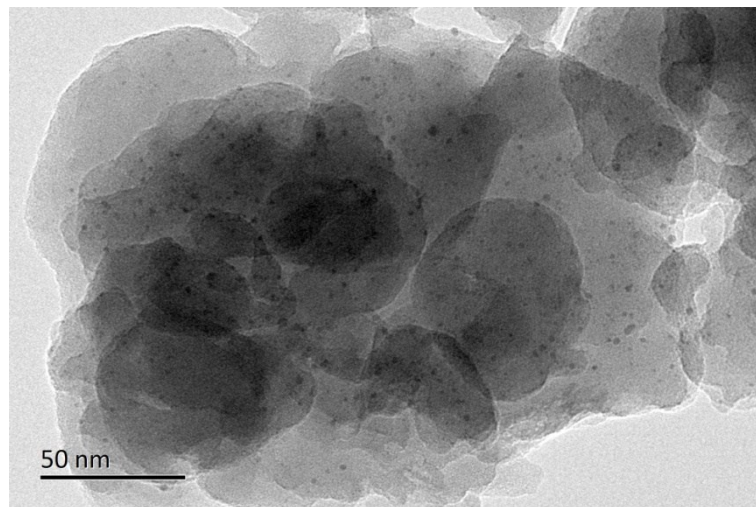


Fig. S8. TEM image of the Pt/SAPO-11-H1 catalyst.